Applied Constant Gain Amplification in Circulating Loop Experiments

Frank Smyth, Daniel C. Kilper, *Senior Member, IEEE*, Sethumadhavan Chandrasekhar, *Fellow, IEEE*, and Liam P. Barry, *Senior Member, IEEE*

***Abstract*—The reconfiguration of channel or wavelength routes in optically transparent mesh networks can lead to deviations in channel power that may impact transmission performance. A new experimental approach, applied constant gain, is used to maintain constant gain in a circulating loop enabling the study of gain error effects on long-haul transmission under reconfigured channel loading. Using this technique we examine a number of channel configurations and system tuning operations for both full-span dispersion-compensated and optimized dispersion-managed systems. For each system design, large power divergence was observed with a maximum of 15 dB at 2240 km, when switching was implemented without additional system tuning. For a bit error rate of 10^{-3}, the maximum number of loop circulations was reduced by up to 33%.**

***Index Terms*—Applied constant gain, circulating loop, EDFA gain dynamics, erbium-doped fiber amplifier (EDFA), reconfigurable WDM networks, simulated constant gain, optically transparent mesh networks, WDM channel power deviation.**

I. Introduction

RECONFIGURATION of channel routing in optically transparent mesh networks adds flexibility by allowing wavelength re-routing for applications such as dynamic link capacity allocation and optical mesh restoration. Key hardware required for automatic reconfiguration of channels, such as reconfigurable optical add/drop multiplexers (ROADMs) and photonic cross connects (PXCs), has been deployed [1]; however, the network automation and optimization techniques required to fully exploit this hardware remain a challenge. One important issue is the performance impact of channel power deviations after reconfiguration caused by loading-dependent gain variation in the erbium-doped fiber amplifiers (EDFAs) and the adjustment histories of network tuning elements.

Manuscript received April 09, 2009; revised June 08, 2009. First published June 19, 2009; current version published September 10, 2009. This work was supported in part by Science Foundation Ireland SFI through the Centre for Telecommunications Value Chain Research (CTVR).

F. Smyth and L. P. Barry are with the School of Electronic Engineering, Dublin City University, Glasnevin, Dublin 9, Ireland (e-mail: smythf@eeng.dcu.ie; barryl@eeng.dcu.ie).

D. C. Kilper is with the Transmission Systems and Networks Research Department, Bell Laboratories, Alcatel-Lucent, Holmdel, NJ 07733 USA (e-mail: dkilper@alcatel-lucent.com).

S. Chandrasekhar is with Bell Laboratories, Alcatel-Lucent, Holmdel, NJ 07733 USA (e-mail: sc@alcatel-lucent.com).

Color versions of one or more of the figures in this paper are available online at http://ieeexplore.ieee.org.

Digital Object Identifier 10.1109/JLT.2009.2025606

EDFAs, commonly used in transparent mesh networks, are operated in saturation to increase efficiency and performance [2]. Due to the resulting cross-gain saturation, channel reconfiguration in transparent networks can create transient power excursions. Depending on the design of the amplifier control and the magnitude of the event, these excursions may last milliseconds or longer. For the worst case of unplanned channel loss due to network failures, the positive or negative power excursions in the surviving channels can potentially lead to transmission errors. The control and impact of such gain transients have been extensively studied [3]–[5]. In networks, rather than maintaining constant output power in the EDFAs, the total gain can be kept constant to prevent instabilities associated with strong channel power coupling due to constant power operation [6]. However, changes in the loading conditions can still result in wavelength-dependent transient and steady-state gain variations on the surviving channels [7], [8].

After transient fluctuations subside, an EDFA will typically settle to a steady-state gain condition that depends on the new channel loading condition. In this paper, we study the impact on transmission performance resulting from this steady-state gain variation caused by channel route reconfiguration. Although steady-state transmission for 10 Gb/s on-off keying WDM signals is well understood, the channel power evolution and corresponding transmission performance in the presence of channel route reconfiguration in transparent networks [9], [10] have not been widely studied for long-haul systems.

The wavelength-dependent gain of an EDFA can be reduced using a gain equalization filter (GEF), which is optimized for a specific channel loading such as uniform or full loading [11]. Residual gain ripple, often on the order of 1 dB or less, and diminished GEF effectiveness due to non-uniform channel loading, can result in significant wavelength-dependent gain error [8]. Spectral hole burning (SHB) can cause further gain variations dependent on the local channel configuration, particularly near the short wavelength EDFA gain peak [12].

Through a chain of EDFAs these effects can be additive and can lead to a large power divergence between channels [13]. Channels that experience low gain can suffer from performance penalties related to poor OSNR or due to crosstalk from higher power neighbors, while channels in a high-gain region of the spectrum can suffer from penalties due to fiber non-linearities.

As transparent networks move toward automatic self-reconfiguration, it is important that issues that may arise in reconfiguration are thoroughly studied. Proposals to implement dynamic wavelength routing in core networks [14] must address the physical limitations imposed by the underlying transmission

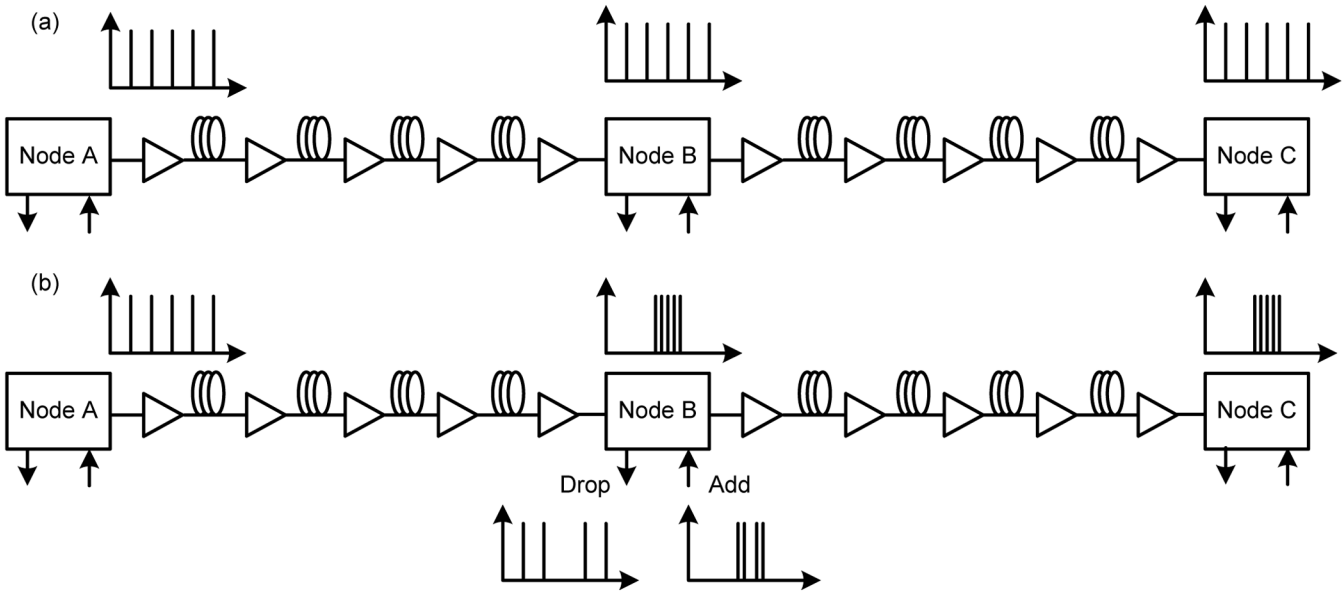

Fig. 1. Example of channel reconfiguration in a long-haul network, showing the scenario (a) before and (b) after the reconfiguration event.

systems. In this paper, we study the effect of reconfiguration on transmission performance for channel configurations such as a five channel waveband and five channels spread uniformly across the C-band. These channel configurations were chosen because they represent some of the extreme channel configurations that may be encountered in a mesh network and therefore give some insight into worst case scenario performance. We use the applied constant gain (ACG) method [13] in a circulating loop to study the performance of uniformly spread and banded channel configurations in systems designed using both full-span dispersion compensation and optimized dispersion management.

II. Power Control and Optimization in Reconfigurable Mesh Networks

Fig. 1 illustrates an example of the reconfiguration event being studied. Three nodes, labeled A to C constitute a section of a mesh network. Each node is separated by four fibre spans with EDFAs to overcome the span losses. Prior to a reconfiguration request, five wavelengths are in place between Node A and Node C. At some point in time, the network operator decides to drop four of these wavelengths at Node B and to add four new wavelengths. The ROADM switches are reconfigured, resulting in the spread configuration from node B to node C becoming a banded configuration. We consider three phases to the re-optimization of the network that will occur after such a channel reconfiguration, and these phases along with associated spectra are depicted in Fig. 2.

— *Phase 1.* Immediately following a channel reconfiguration the fast control circuits of the EDFAs automatically adjust the pumps in order to maintain constant gain and reduce transient gain excursions. It should be noted that some transient power fluctuations may still occur prior to the steady state being reached but because the effects are on very fast timescales ($\sim$ microsecond) they are not considered here.

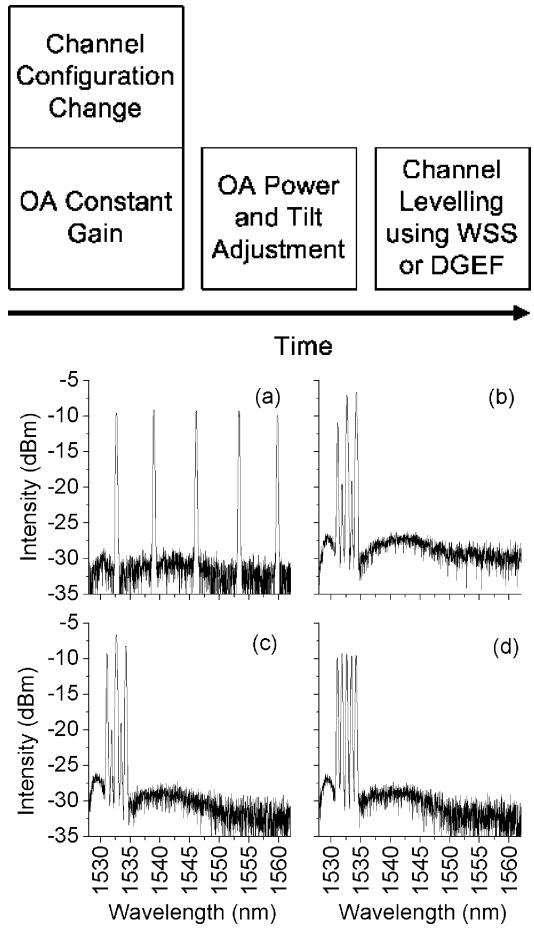

Fig. 2. (Above) Three phases of optimization after channel reconfiguration. (Below) Spectra representing the reconfiguration and re-optimization process; (a) prior to reconfiguring; (b) after constant gain is applied; (c) after power and tilt is retuned; (d) after fine tuning.

— *Phase 2.* While the constant gain operation serves to reduce gain transients, it can also cause EDFAs to deviate

from their target output powers. The second phase occurs on a slower timescale than phase 1 and consists of adjustments to the EDFA pumps and variable optical attenuators (VOAs) in order to return to the target output power and spectral tilt.

— *Phase 3.* The third phase is a fine tuning phase in which residual gain ripple is leveled out using gain leveling controls such as per-channel VOAs found in ROADM wavelength-selective switches (WSSs). These slow network tuning elements will be adjusted depending on the details of the new configurations and the pre-existing or historical settings of the tuning elements.

Note that this method examines the fastest possible network reconfiguration procedure, in which all switches are immediately switched to the new configuration. It is likely in practice that reconfiguration would involve gradually turning down power in the channels being removed and then gradually turning up power in the channels being turned on. This procedure may also require additional sequencing of operations in order to avoid power instability or even oscillation [15]. Thus, the approach used here probes the limitations on reconfiguration imposed by the long time scale or steady-state network tuning requirements and does not consider the limits due to fast tuning requirements.

III. Representing Mesh Networks With Circulating Loops

In the laboratory, long-haul networks are often studied using a circulating loop [16]. In such experiments a number of amplified spans are used repeatedly to yield transmission characteristics typical of long-haul systems, while using the hardware of only a few spans. Circulating loop experiments to study reconfigurable optically transparent mesh networks are more complicated than their point-to-point counterparts due to the number of different combinations of available route parameters [17]. In addition, the amplifiers in a circulating loop are normally operated with constant output power (or constant pump power) in order to maintain stability in the loop. This contrasts with the constant-gain regime generally used in mesh networks and poses a challenge for the accurate study of system performance.

In [18] the authors use constant gain control in a four channel circulating loop using custom high-speed control. This configuration requires careful matching of the gains and losses in the loop and is prone to instability. Any power deviation at the amplifier output will propagate around the loop and, due to the constant gain condition, will grow or diminish until the amplifier power limits are reached or in some cases destabilize the control loop. In addition, it may be difficult to differentiate between effects caused by the using constant gain control in the loop and transmission effects related to constant gain amplification.

In this work we present the ACG technique based on methods used in [13], which allows the constant-gain scenario to be accurately represented in a stable constant-power operated circulating loop. Prior to reconfiguration, we measure the gain in each of the constant-power mode loop amplifiers. Once the reconfiguration is complete, we measure the new input powers to the amplifiers and apply the measured gains by setting a new constant output power. As a change to any EDFA affects every other EDFA this is an iterative process performed until all gains are within 0.5 dB of the measured gain.

In order to study the impact of the power deviation caused by reconfiguration, the scenario illustrated in Fig. 1 was used. A loading condition consisting of five channels spread uniformly across the spectrum was reconfigured to a loading condition of five channels grouped together in a waveband with performance measured before reconfiguration, after reconfiguration, and also after Phase 2 and Phase 3 re-optimization. The low channel counts used in spread and banded configurations represent some extreme channel configurations that may occur and hence give some insight into possible worst case scenarios, however, as the number of channels in a given band or configuration increases, wavelength-dependent gain tends to get averaged and larger channel counts tend to have a stabilizing effect. For example, the removal of five channels from a 40-channel configuration will have little impact on the other 35 channels. In this case the largest effect is likely to be associated with changes in the spectral hole burning profile near the 1535 nm gain peak. It should also be noted, however, that with large numbers of channels, the impact of Raman scattering becomes more pronounced and tilt variations may still be important when reconfiguring among different configurations with large channel counts [13].

IV. Experiment

A. Setup

The circulating loop setup shown in Fig. 3 was used throughout the experiment. Forty 100 GHz-spaced channels were generated using distributed feedback (DFB) lasers and multiplexed together. One tunable 300-pin multisource agreement (MSA) standard 10.7 Gb/s non-return-to-zero on-off keyed (NRZ-OOK) transceiver was tuned to the channel of interest and inserted in place of the corresponding DFB to yield a 40-channel data modulated comb. All channels were modulated with a $2^{31} - 1$ bit pseudorandom bit sequence (PRBS). An optical switch allowed the tunable transmitter to be replaced with a continuous wave (CW) external cavity laser (ECL) for optical signal-to-noise ratio (OSNR) measurements.

The modulated channels were amplified using the first of seven commercial JDSU line amplifier modules used in the experimental testbed. These two-stage EDFAs are designed for use in commercial DWDM systems with specifications typical for metro regional and long-haul networks including: 27 dB gain design point, 5.8 dB noise figure, ± 0.75 dB maximum gain variation and $+22$ dBm nominal output power. They had two pumps per stage and midstage VOAs for tilt adjustment.

Although the details of the effects observed, such as the wavelength dependence, will vary depending on the specific gain characteristics of the amplifiers, similar effects are expected from other gain-flattened DWDM line amplifiers and have been observed in separate measurements (not shown here) on different makes and models of EDFAs.

The EDFA modules offered three modes of operation: constant gain, constant pump current and constant output power. The input EDFA, being outside of the loop, was operated in constant gain mode. A WSS at its midstage had two functions: to set up the desired channel configuration by blocking the

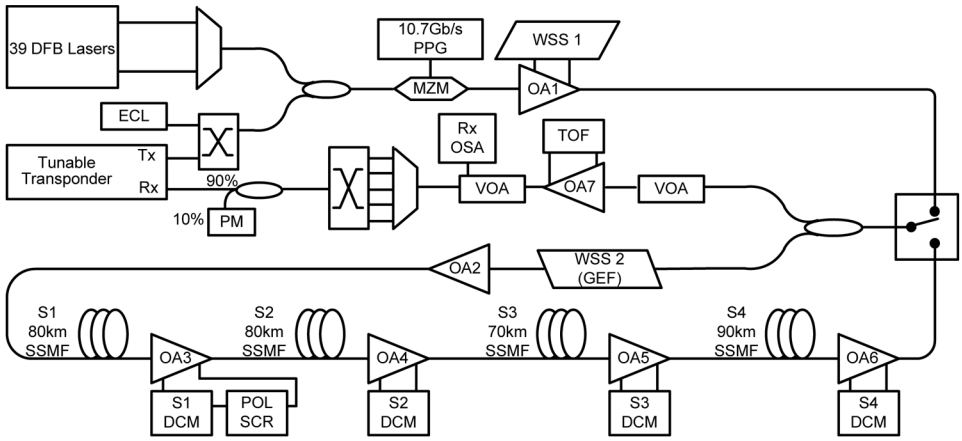

Fig. 3. Schematic of the experimental setup. (OA) Optical amplifier; (WSS) wavelength selective switch; (TOF) tunable optical filter; (DCM) dispersion compensation module; (POL SCR) polarization scrambler; (PM) power meter; (VOA) variable optical attenuator; (OSA) optical spectrum analyzer; (PPG) pulse pattern generator; (SSMF) standard single-mode fiber.

unwanted channels and to level the input channels such that their individual power levels remained constant regardless of the configuration.

The loop consisted of four amplified spans of standard single-mode fiber (SSMF). The nominal spans lengths were 80, 80, 70, and 90 km, respectively, and the average span loss, including splices, taps, attenuators, and switches [19] was 25.8 dB. The EDFAs inside the loop were also two-stage EDFAs. Dispersion compensation modules (DCMs) were inserted midstage in each EDFA and a polarization scrambler was also placed in line with the first DCM. An additional two-stage EDFA was placed before the first span to compensate for component losses between the transmitter and the first span. Each of these loop EDFAs was used in constant output power operation mode, in which the output power of the amplifier was actively held constant by adjustment of the pump power. A second WSS used inside the loop acted as a dynamic GEF, providing pre-emphasis to level out the additive ripple of the five loop amplifiers. It was located at the beginning of the loop to represent its position on the add side of a ROADM in an east-west separable node and was adjusted in order to give a flat and level spectrum at its own input at all times. This ensured that the loading and looping channels experienced the same filtration. At low channel powers the ASE in the loop grew rapidly. In addition to its role as a GEF, this WSS was also used to block ASE in the unoccupied channel locations.

At the output of the loop the OSNR was varied by attenuating the signal power at the input to OA7, while maintaining constant output power from the EDFA. A 5 nm tunable optical filter in the midstage of the output EDFA was used to reduce the amplified spontaneous emission (ASE) and signal power away from the channel of interest. A second VOA was used at the output of OA7 to adjust the power falling on the receiver and a tap on this VOA was connected to a calibrated optical spectrum analyzer (OSA) that was used for OSNR measurements. The signals were demultiplexed using a 100 GHz arrayed waveguide grating (AWG) based demultiplexer. An optical switch placed after the demultiplexer was used to direct the channel of interest to the receiver of the MSA transponder via a calibrated power meter. For the required OSNR measurement, the receiver power

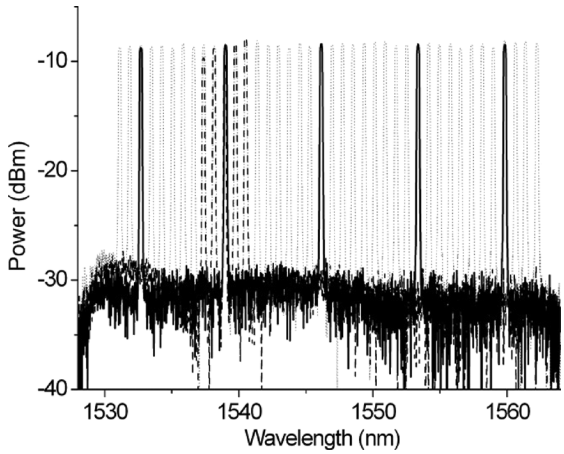

Fig. 4. Three of the configurations used. The dotted gray spectrum shows configuration 1. The solid black line shows configuration 2, and the dashed black line shows configuration 4.

was maintained at -13 dBm while the OSNR was degraded until a bit error rate (BER) of 1×10^{-3} was reached. The OSNR was then calculated using a measurement of the peak power of the channel of interest, along with an averaged noise measurement taken either side of a CW external cavity laser that was inserted in place of the modulated channel and carefully adjusted to the corresponding power level. This method enabled accurate OSNR measurements in the presence of ROADM passband filtering. The required OSNR measurement, along with the delivered OSNR at the exit of the loop was taken for each round trip.

B. Channel Configurations

Configuration 1 consisted of forty 100-GHz spaced C-band channels. Configuration 2 consisted of five of these channels spread uniformly across the C-band. The wavelengths of these channels were 1532.68, 1538.98, 1546.12, 1553.33, and 1559.79 nm. Configurations 3–7 consisted of a band of five channels with one of the channels from Configuration 1 as the center channel together with its four closest neighboring channels. Three of the configurations are shown in Fig. 4 after

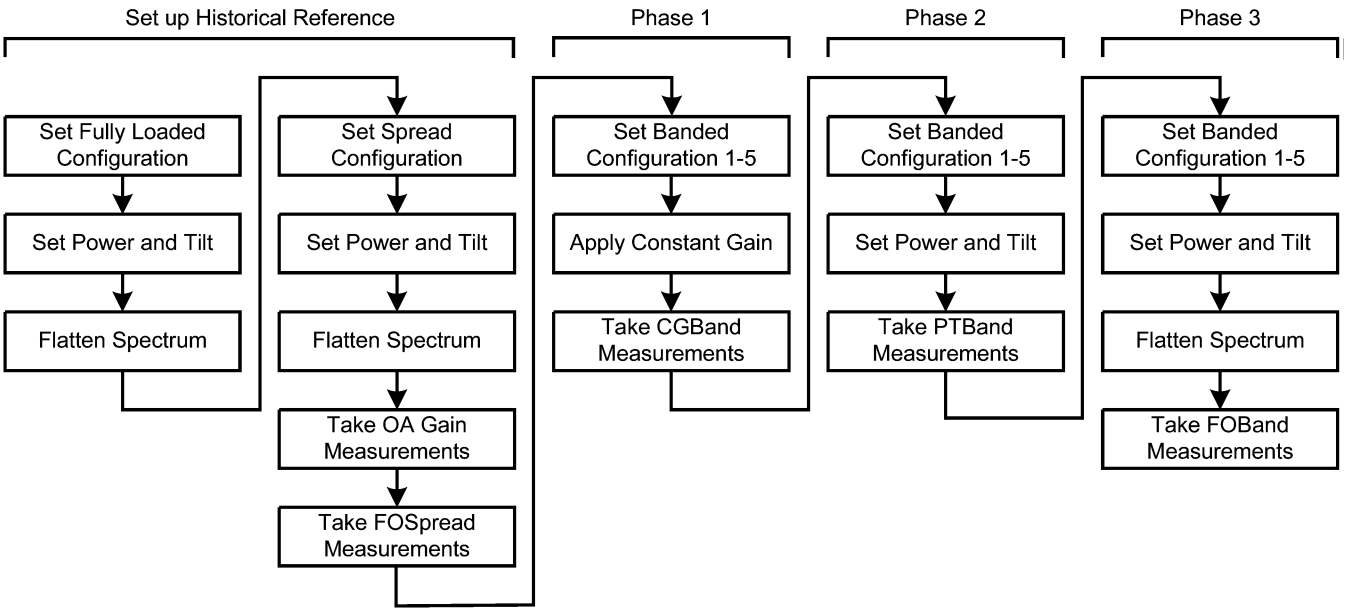

Fig. 5. Flow chart depicting the experimental process. Phase 1 measurements are taken for configurations 3 to 7 before moving to Phase 2 measurements.

one round trip. A performance measurement (required OSNR and delivered OSNR) was taken for each of the five channels of configuration 2, both before and after reconfiguration and also as the system was re-optimized for the new banded configuration.

C. Reference Case

The experimental process is depicted in the flowchart in Fig. 5. The system arrangement (including EDFA and channel leveling settings) that is in place when a channel reconfiguration takes place may have a major impact on the phase 1 performance. For this reason a consistent starting point was used for each measurement. The EDFAs are designed to operate fully loaded so this configuration was used as the reference case. Of course, other reference cases or nominal settings can be used. Each EDFA was set to achieve the desired launch power and spectral tilt for this fully loaded configuration, and the "per-channel" VOAs of the loop WSS were then set to flatten any residual gain ripple. The resulting WSS attenuator settings are displayed in Fig. 6(a). From this reference point the channels were set to configuration 2 (five channels uniformly spread across the band). The reduction from 40 channels to 5 caused a 9 dB drop at the input to the loop so all of the amplifier output powers were reduced by 9 dB to maintain constant gain and the WSS was adjusted to reflatten the spectrum with the new configuration. Note that only the open channels were adjusted as shown in Fig. 6(b), which shows the WSS shape after optimizing configuration 2. It is seen that in order to flatten the spectrum, the attenuation for the shortest wavelength was reduced while the three central channels are attenuated farther indicating that the wavelength-dependent gain has varied significantly despite the total gain remaining constant. This variation arises due to a reduction in Raman tilt with only five channels, suboptimal gain equalization, as well as channel-loading-dependent gain variations caused by gain ripple and tilt and other potential physical effects such as SHB. Note that the attenuation for channel 3 is opposite to the trend that would be expected due to changes in Raman tilt alone and primarily results from changes in the amplifier gain ripple, which may include SHB. Taking the reference setting to be the midpoint for a set of extreme values can at best cut the variation in half. Performance measurements were taken for each of the five channels of the uniformly spread configuration 2 and these results are referred to as "fully optimized for the spread configuration" or "FOSpread." For example, FO1559Spread refers to the Fully Optimized (phase 3 measurements) of the 1559 nm channel when it is part of the uniformly spread configuration.

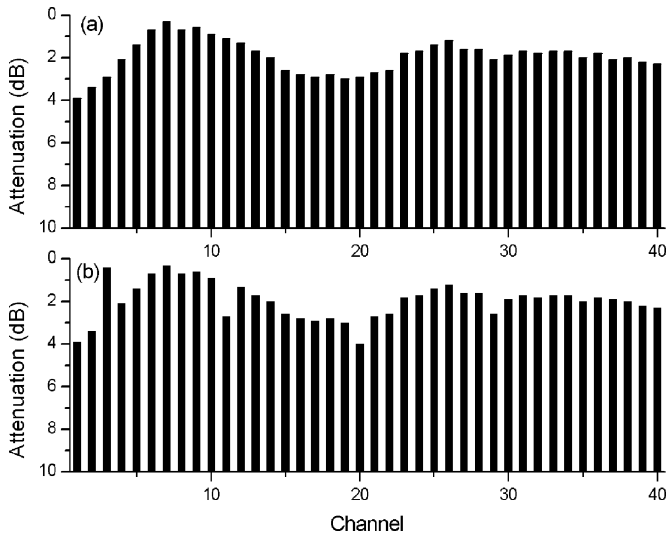

Fig. 6. WSS1 channel attenuations after (a) 40-channel optimization and (b) configuration 1 optimization. Channel 1 is at the shortest wavelength.

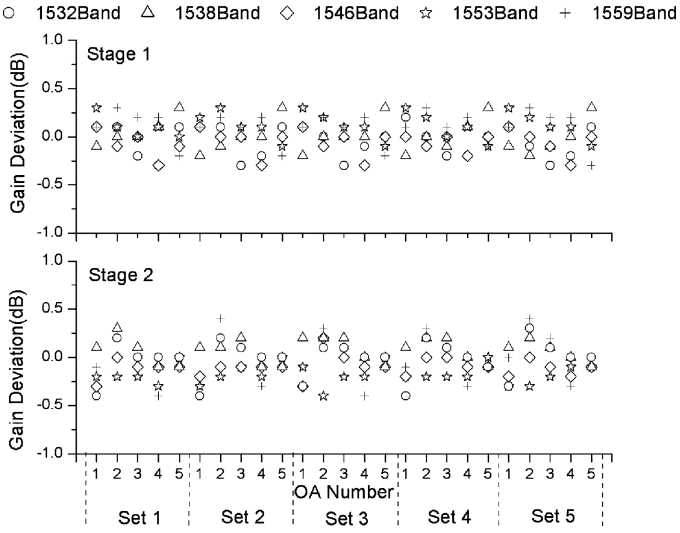

Fig. 7. Measured deviation from target gain for stage 1 and stage 2 of the loop EDFAs after the ACG technique in the 0 dBm launch power case.

D. Phase 1 Measurements: Applied Constant Gain in a Circulating Loop

IIn contrast to a straight line reconfigurable system in which the amplifiers gains are kept constant, we chose to operate the EDFAs in the circulating loop configuration with constant output power for improved stability and reliable behavior.In order to make meaningful measurements on phase 1 of the optimization cycle it was necessary to use the ACG technique described previously on the EDFAs used in the loop.

The power of the loop loading channels was held constant and this, combined with the use of constant gain on the loop loading amplifier ensured that the total input power to the loop remained constant for all five-channel configurations. Inside the loop, however, the non-ideal WSS settings for the new configuration caused the power input to the first EDFA to change. A change in input power to a constant-power controlled EDFA causes its gain, and hence its ripple and tilt to change. This effect propagated through the loop and caused similar gain changes for all of the other amplifiers in the loop. This situation is undesirable as it departs from what would occur in a network operating with constant gain. The EDFA output powers required to revert to the prereconfiguration gain can be calculated by measuring the new input powers to each EDFA. These output powers can then be set while maintaining the stable constant-power mode in the circulating loop. Changes are made iteratively until the gain of each EDFA is within tolerance. As shown in Fig. 7 the algorithm achieved a tolerance of ± 0.4 dB between desired and achieved gain, both for the individual EDFA stages and for total EDFA gain. The EDFA power monitor photodiodes were accurate to ± 0.1 dB. Note that the EDFA power measurements are not gated, and hence each power measurement can represent the power after any number of round trips. For this reason, the rounded average of five individual measurements was taken as the EDFA power measurement. Performance measurements taken at this point of the experiment are referred to as "constant gain for the banded configuration" or "CGBand." For example CG1546Band refers to Constant Gain (phase 1 measurements) of the 1546 nm channel in the banded configuration.

E. Phase 2 and Phase 3 Measurements

As mentioned in the previous section, channel configuration changes can cause variations in the wavelength-dependent gain even if the EDFA control maintains constant total power gain. Hence, after a reconfiguration it will often be necessary to adjust the amplifiers to return to the desired launch powers and total spectral tilt. In this work, Phase 2 of the network re-optimization process involved readjusting the EDFAs output power and tilt. In a circulating loop a change to any amplifier affects all of the amplifiers, so this was an iterative process, repeated a number of times (depending on the system) until a steady-state was reached with all amplifiers in tolerance. Performance measurements taken after phase 2 re-optimization are referred to as "power and tilt for the banded configuration" or "PTBand."

Note that up to this point the per-channel leveling shape has not been adjusted for the new channel configuration and remains as shown in Fig. 6(b), optimized for configuration 2. Clearly this arrangement is non-ideal for the waveband configurations 3-7. Phase 3 of the re-optimization process consisted of iteratively adjusting the power and tilt of the EDFAs, and the channel power tuning elements of the WSS in order to get a flat spectrum with all channels at the desired mean channel power. Performance measurements taken at this point of the experiment are referred to as "fully optimized for the banded configuration" or "FOBand."

F. Channel Launch Powers and Dispersion Maps

The full measurement process was performed using four different per-channel launch powers (0, 2, 4, and 6 dBm). Return-to-zero dispersion maps (in which the DCMs and span lengths were nominally matched) were used for the 0 and 2 dBm cases. The use of higher launch powers of 4 and 6 dBm required an optimized dispersion map to control non-linear effects. Precompensation of -500 ps/nm was used in addition to a singly periodic dispersion map with a residual dispersion per span (RDPS) of 34 ps/nm.

V. Analysis of Results

A. Power Evolution

While circulating loops offer the ability to examine transmission performance at long-haul distances in the laboratory, they have by their nature, the potential to exaggerate the impact of certain effects due to identical components being traversed many times. However, if the amplifiers used in a system have similar architectures, including gain flattening filters, then the response through a loop may be similar to that of a straight line system.

In networks that employ constant gain, the EDFAs will generally be set for a desired launch power and then run with constant gain control. The launch power may be calculated simply as the desired mean channel power multiplied by the number of channels; alternatively, more complicated calculations involving the known noise figures of the amplifiers may be used in order to

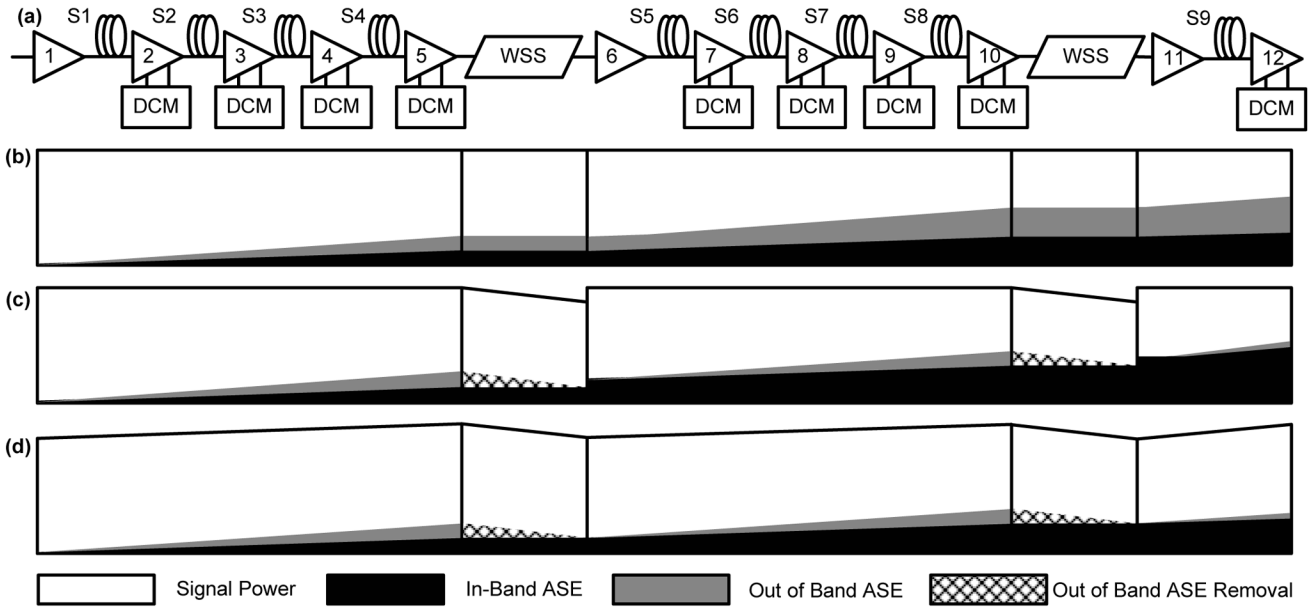

Fig. 8. Power evolution in a straight line system. (a) Block diagram of the straight line system. (b) No ASE filtering. (c) Total output power method of amplifier adjustment. (d) Mean channel power method of amplifier adjustment.

predict and account for the ASE growth. In reconfigurable networks however, the addition of channels with varying histories can reduce the effectiveness of precalculated methods.

It was important to ensure that the power evolution of our loop system represented that of a straight line system. In this work, two methods of power control (first identified in [20]) were examined initially and these are illustrated in Fig. 8. The solid white boxes represent the power in the channels, the dark gray areas represent out of band ASE and the solid black areas represent in-band ASE. The hatched areas represent out of band ASE removal by the WSS.

Fig. 8(a) shows the straight line system being represented, with nodes (represented in our experiment by the WSS) linked by four amplified spans. Fig. 8(b) illustrates how the OSNR degrades if the WSS is not used to filter ASE by closing unused ports. With the low channel counts used in our experiment the ASE grew rapidly. Fig. 8(c) illustrates a method of power control in which the EDFA output power is simply set to match a target. In contrast, for the method illustrated in Fig. 8(d), it is set such that the power in the channels alone (out-of-band ASE power was ignored) matched a target. The total power method of Fig. 8(c) is faster because an EDFA photodiode power reading will suffice, whereas the channel power method of Fig. 8(d) requires a spectrum analyzer sweep to calculate the power in the channels. However, with the total power method, the out of band ASE growth is not taken into account and as the ASE grows, the power in the channels is reduced proportionally and the OSNR is degraded. Conversely with the channel power method, the additional power added to keep the mean channel power constant means that the OSNR degradation due to ASE growth is less severe. Due to its superior resilience to OSNR degradation this method was used throughout the experiment.

The total power immediately after WSS2 will be approximately equal to the total power in the channels alone because the majority of the out of band ASE has been removed by the WSS. Power measurements for each round trip, taken at the output of the WSS while recirculating confirmed that the power evolution of a straight line system using the power control method of Fig. 8(d) was being accurately represented. For the cases with per-channel launch powers of 4 and 6 dBm a drop in channel powers of up to 1.2 dB was measured after nine round trips while the total power remained constant. For the lower launch power cases of 0 and 2 dBm a channel power drop of up to 0.5 dB after five round trips was observed.

B. Transmission Performance

The delivered OSNR and the OSNR required to achieve a BER of 1×10^{-3} were taken for the channel in question after each round trip. These, together with the OSNR margin (the difference between delivered and required OSNRs) were used to evaluate the transmission performance for the various channel configurations and launch powers. Fig. 9 shows the required OSNR measurements as a function of distance for the 6 dBm launch power and the 2 dBm launch power. The highlighted plots correspond to the four reconfiguration and re-optimization scenarios for the 1559 nm channel. The first point of note is that the 6 dBm per-channel launch power allows for a greatly extended reach. In some cases the reach is twice that of the 2 dBm launch power. The reason for this is the optimized dispersion map, which, as is well known [21], enables high launch powers while keeping non-linear distortion low. The effect of the dispersion map can be seen by the difference in the shape of the 6 dBm curves when compared to the 2 dBm curves. In Fig. 9(a) it is seen that the required OSNR for all channels stays quite constant for the first five round trips. In contrast, Fig. 9(b) shows that despite the lower launch power, the required OSNR increases from the outset and many of the channels cannot reach five round trips with an acceptable BER even when fully optimized.

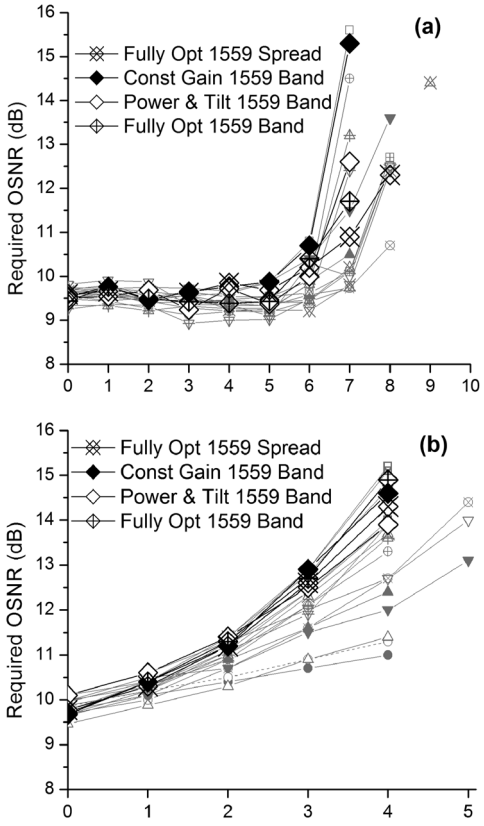

Fig. 9. Required OSNR as a function of distance for (a) 6 dBm launch power and (b) 2 dBm launch power as a function of number of round trips.

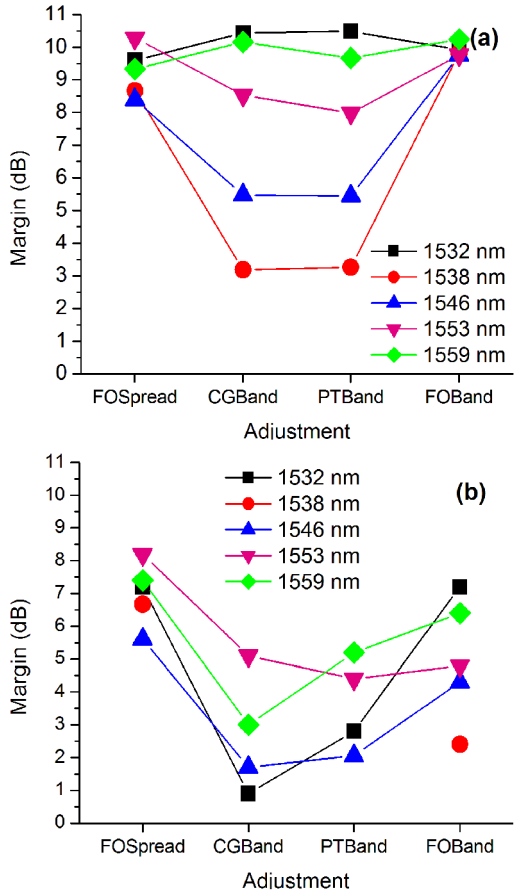

Fig. 10. Margin after (a) 1600 km and (b) 2240 km for each adjustment step with 6 dBm launch power.

Another interesting point to note from Fig. 9(a) is the role played by the reconfiguration and subsequent re-optimization. Looking at the highlighted 1559 nm channel after seven round trips it can be seen that the required OSNR varied substantially for each of the scenarios. At this distance the initial configuration of FO1559Spread exhibits a required OSNR of 10.9 dB. When the configuration changes from spread to banded and constant gain is applied, the required OSNR increases dramatically to 15.3 dB, which based on power measurements is consistent with an increase in non-linear penalties. Phase 2 optimization involves re-optimizing the power and tilt of the EDFA and results in a 2.7 dB improvement in required OSNR to 12.6 dB. When the WSS is adjusted for the new configuration in phase 3, a further 0.9 dB improvement is achieved bringing the required OSNR to 11.7 dB.

Similar reconfiguration and re-optimization data are presented in Fig. 10. The 6 dBm launch power OSNR margins are shown for each of the five channels at five round trips or 1600 km [Fig. 10(a)] and seven round trips or 2240 km [Fig. 10(b)]. At 1600 km the 1532 and 1559 nm channels experience a slight benefit when reconfigured, whereas the margin is reduced by up to 5.5 dB for the other channels. Despite this penalty, each channel maintains a margin of at least 3 dB to this distance. Little improvement is registered after tuning the power and tilt of the amplifiers, but when the channel powers are fine tuned using the WSS, FOBand margins recover to within 1 dB of the FOSpread in the worst case. From Fig. 9(a), it is apparent that the required OSNR at this distance is constant to within 1 dB; therefore larger margin variations are due to the delivered OSNR. The 2.5 dB range of margins for the FOSpread case are indicative of the impact of wavelength-dependent gain ripple within the system. The small margin variations among the FOBanded cases demonstrate that the power is accurately and reproducibly set during the system tuning and using the applied constant gain method.

At 2240 km, all of the channels suffer a margin penalty when reconfigured; in fact at this distance the 1538 nm channel has a delivered OSNR that is lower than its required OSNR indicating that transmission with a BER of 1×10^{-3} is not possible for all but the fully optimized cases. This behavior is a complex mixture of factors impacting both delivered and required OSNR. After full optimization, the behavior of the network will be more predictable due to the fact that all channels will be leveled to a known power, however, full optimization does not necessarily improve performance. In some cases [see Fig. 10(a)], channels with constant gain applied outperformed those that had undergone phase two and/or phase three optimization. In these cases the channels in question benefited somewhat when the imparted power deviations moved them to a higher power and thus improved OSNR. This benefit, however, may come at the expense of neighboring channels or result in worse performance over long distances as exhibited in Fig. 10(b).

A number of factors that can affect the postreconfiguration performance are evident from Fig. 11, which shows the

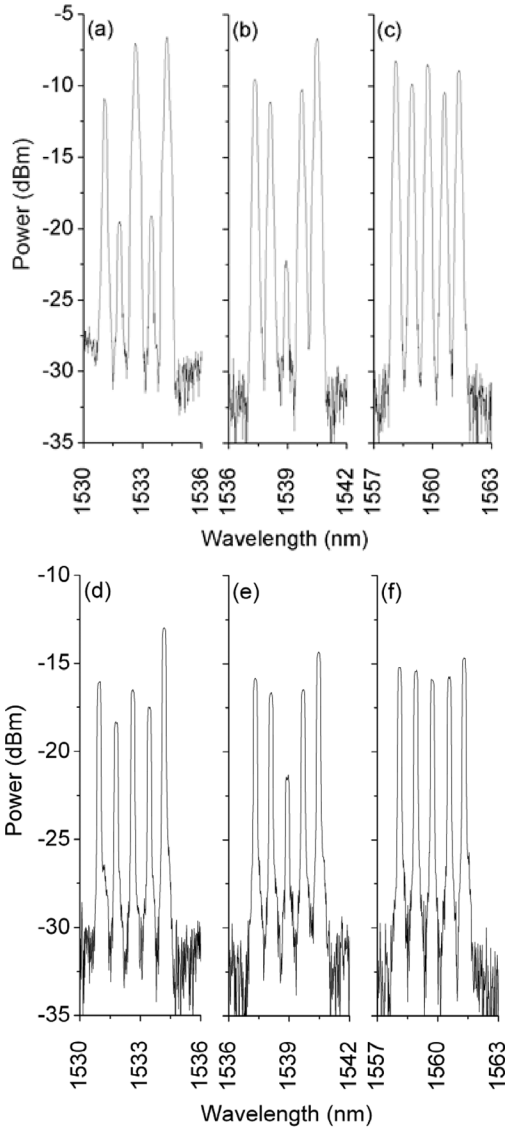

Fig. 11. Spectra after seven round trips with the 6 dBm per-channel launch power for (a) CG1532Band, (b) CG1538Band, and (c) CG1559Band and spectra after four round trips with the 0 dBm per-channel launch power for (d) CG1532Band, (e) CG1538Band, and (f) CG1559Band.

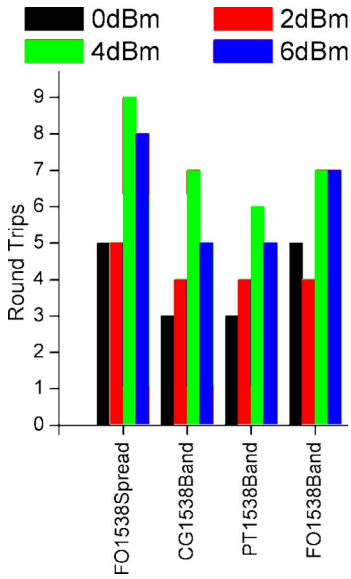

Fig. 12. Number of round trips completed for each configuration using four different launch power levels.

optical spectra after reconfiguration for the CG1532Band, CG1538Band, and CG1559Band at a distance of seven round trips for the 6 dBm launch power [(a), (b) and (c)] and four round trips for the 0 dBm launch power [(d), (e) and (f)]. For the 6 dBm case a channel power divergence of up to 15 dB can be seen in the CG1538Band spectrum. The attenuation profile of the WSS shown in Fig. 6(b) correlates with these spectra. It is seen that for the 1532 nm channel the level of attenuation has been lowered in order to level the uniformly spread configuration and this results in a high-powered central channel in the waveband configuration. For the 1538 nm channel the attenuation has been increased and so the power in the central channel degrades rapidly with distance. These effects will lead to non-linearity-related and low OSNR-related penalties respectively. In contrast, the 1559 nm channel does not require much change in attenuation in order to level the uniformly spread spectrum; hence even at a distance of 2240 km the power divergence for CG1559Band is only 3 dB. It can be seen from Fig. 10(b) that at this distance the 1559 nm channel outperforms both the 1532 and 1538 nm channels. As indicated by Fig. 11(d)–(f), similar power divergence was found for all of the different launch powers, which is further evidence that the power divergence cannot be attributed to Raman tilt alone, since the Raman tilt should be significantly reduced at the lower launch powers [10].

Evidence of SHB can be seen in the spectra of Fig. 11. If the effects of the WSS on the central channels are ignored, a hole in the gain profile around the central channel can be seen. Despite only the central channels of the waveband having been adjusted with the WSS, a large power divergence is also seen on the adjacent channels, and while performance measurements were not taken for these adjacent channels, trends similar to that observed on the measured channels would be expected. Consistent with the influence of SHB, the effect is more prominent for the short wavelength bands such as those at 1532 and 1538 nm than for the 1559 nm band.

Fig. 12 compares the number of round trips completed with finite margin (i.e., > 0) by the 1538 nm channel for the four different launch powers. Note that the reach is only counted in discrete steps of one round trip and the OSNR margin at each distance is not considered. For most of the channels that were measured the variation in reach caused by reconfiguration and re-optimization was at most a single round trip. The exception to this was the 1538 nm channel in which reach reduction of up to 33% (three round trips) was observed after reconfiguration with the 6 dBm launch power. This was caused by the severe reduction in delivered OSNR caused by the large WSS attenuation required to level the spectrum for the uniformly spread case. Considering the case of Fig. 1 where 4 of the 5 channels in Configuration 1 required re-routing, but the 1538 nm channel was to stay on its current path, a configuration change from uniformly spread to banded for this purpose causes an initial reduction in possible transmission distance of almost 1000 km for the

1538 nm data channel. In practice, these variations can be addressed by implementing wavelength re-routing in incremental steps and providing additional margins. Thus, reconfiguration speed and transmission margin are two design details that potentially can be traded in dynamic networks.

VI. Conclusion

In this paper we have provided a first examination of the impact of wavelength reconfiguration on transmission performance over long-haul distances. Large wavelength-dependent penalties were accrued due to channel power deviation caused by steady-state gain dynamics in the EDFAs and the historical arrangement of network tuning elements. Per-channel power tuning was required to achieve satisfactory performance in all cases. These issues complicate or limit the potential for achieving fast wavelength re-routing in long-haul core networks.

The constant-power condition required for stable operation of EDFAs in a circulating loop hinders the study of these reconfiguration related performance issues in a laboratory environment. We introduced the ACG technique that enables the in-depth study of performance during the reconfiguration event and the subsequent re-optimization of the network for the new configuration. Although channel power evolution representative of constant gain amplified systems was observed, as with any circulating loop experiment additional measurements comparing results with a straight line system are needed to give a quantitative evaluation for a particular system.

Results showed that in the ACG circulating loop system, after reconfiguration, a channel's transmission reach at an FEC limit of 10^{-3} could shorten by up to 33% prior to re-optimization. Measurements including systems with precompensated as well as return-to-zero dispersion maps over a range of common channel launch powers revealed a complex array of performance responses to wavelength reconfiguration. Moving to lower channel power did not significantly reduce the power divergence, although the impact on reach was limited by the already poor transmission performance. Higher channel powers with in-line dispersion management leads to better overall performance, both before and after reconfiguration. Only a few of the numerous possible wavelength configurations were considered, however, these cases give an indication of the range of different effects that must be considered. Low channel counts were examined to probe some of the worst case scenarios. Although the wavelength-dependent gain effects should decrease with larger channel counts, other configuration dependant effects such as Raman scattering may increase and impact the performance. Further study of these and other reconfiguration-related performance issues will be aided by the use of the described ACG technique.

References

[1] P. Morkel, Edge-to-core optical switching in Metro apps. Jan. 2008., accessed Jul 6, 2009. [Online]. Available: http://lw.pennnet.com/display_article/321314/63/ARTCL/none/none/1/Edge-to-core-optical-switching-in-metro-apps/

[2] E. L. Goldstein, L. Eskildsen, C. Lin, and R. E. Tench, "Multiwavelength propagation in lightwave systems with strongly inverted fiber amplifiers," *IEEE Photon. Technol. Lett.*, vol. 6, no. 2, pp. 266–269, Feb. 1994.

[3] F. Shehadeh, R. S. Vodhanel, C. Gibbons, and M. Ali, "Comparison of gain control techniques to stabilize EDFA's for WDM networks," presented at the POFC'96, .

[4] M. I. Hayee and A. E. Willner, "Transmission penalties due to EDFA gain transients in add-drop multiplexed WDM networks," *IEEE Photon. Technol. Lett.*, vol. 11, no. 7, pp. 889–891, Jul. 1999.

[5] D. Kilper, C. Chandrasekhar, and C. A. White, "Transient gain dynamics of cascaded erbium doped fiber amplifiers with re-configured channel loading," presented at the Proc. OFC/NFOEC'06, .

[6] S. J. B. Yoo *et al.*, "Observation of prolonged power transients in a reconfigurable multiwavelength network and their suppression by gain-clamping of optical amplifiers," *IEEE Photon. Technol. Lett.*, vol. 10, pp. 1659–1661, 1989.

[7] J. L. Zyskind *et al.*, "Fast power transients in optically amplified multi-wavelength networks," presented at the Proc. OFC'96, .

[8] D. C. Kilper, C. A. White, and S. Chandrasekhar, "Control of channel power instabilities in constant-gain amplified transparent networks using scalable mesh scheduling," *J. Lightw. Technol.*, vol. 26, no. 1, pp. 108–113, Jan. 2008.

[9] D. C. Kilper and C. A. White, "Fundamental saturated amplifier channel power dynamics in transparent networks," in *Proc. ECOC*, 2005, pp. 693–694.

[10] D. C. Kilper, F. Smyth, L. Barry, and S. Chandrasekhar, "Power divergence due to wavelength re-routing in long haul circulating loop experiments," in *Proc. ECOC*, 2008, pp. 1–2.

[11] A. Srivastava and Y. Sun, "Advances in erbium doped fiber amplifiers," in *Optical Fiber Telecommunications*, I. P. Kaminow and T. Li, Eds. San Diego, CA: Academic, 2002, vol. IVA.

[12] G. Luo, J. L. Zyskind, J. A. Nagel, and M. A. Ali, "Experimental and theoretical analysis of relaxation-oscillations and spectral hole burning effects in all-optical gain-clamped EDFA's for WDM networks," *J. Lightw. Technol.*, vol. 16, no. 4, pp. 527–533, Apr. 1998.

[13] C. Fürst *et al.*, "Impact of spectral hole burning and raman effect in transparent optical networks," presented at the Proc. ECOC, 2003.

[14] J. M. Yates, M. P. Rumsewicz, and J. P. R. Lacey, "Wavelength converters in dynamically-reconfigurable WDM networks," in *IEEE Communications Surveys and Tutorials*, Second Quarter 1999, vol. 2, no. 2, pp. 2–15.

[15] D. C. Kilper, C. A. White, and S. Chandrasekhar, "Control of channel power instabilities in transparent networks using scalable mesh scheduling," presented at the Proc. OFC/NFOEC, 2007.

[16] N. S. Bergano and C. R. Davidson, "Circulating loop transmission experiments for the study of long haul transmission systems using erbium-doped fiber amplifiers," *J. Lightw. Technol.*, vol. 13, no. 5, pp. 1553–1561, May 1995.

[17] S. Chandrasekhar and D. Kilper, "Using testbeds for optically-transparent mesh network experimentation," in *Proc. LEOS*, 2006, pp. 771–772.

[18] T. Yoshikawa, K. Okamura, E. Otani, T. Okaniwa, T. Uchino, M. Fukushima, and N. Kagi, "WDM burst mode signal amplification by cascaded EDFAs with transient control," *Opt. Express*, vol. 14, pp. 4650–4655, 2006.

[19] D. Kilper, S. Chandrasekhar, E. Burrows, L. Buhl, and J. Centanni, "Local dispersion map deviations in metro-regional transmission investigated using a dynamically re-configurable re-circulating loop," presented at the Proc. OFC'07, .

[20] C. R. Giles and E. Desurvire, "Propagation of signal and noise in concatenated erbium-doped fiber optical amplifiers," *J. Lightw. Technol.*, vol. 9, no. 2, pp. 147–154, Feb. 1991.

[21] S. Chandrasekhar and A. H. Gnauck, "Performance of MLSE receiver in a dispersion-managed multispan experiment at 10.7 Gb/s under nonlinear transmission," *IEEE Photon. Technol. Lett.*, vol. 18, no. 12, pp. 2448–2450, Dec. 2006.

Frank Smyth received the B.Eng., M.Eng., and Ph.D. degrees in electronic engineering from Dublin City University, Dublin, Ireland, in 2001, 2003, and 2009, respectively.

In 2007, he was awarded the Bell Labs Summer Internship Grant and spent six months working with the Optical Networks Research Department, Bell Laboratories, Alcatel-Lucent, Holmdel, NJ. In 2009, he took up a position as a Postdoctoral Researcher with the Radio and Optical Communications Group within the Research Institute for Networks and Communications Engineering (RINCE), Dublin City University. His current research interests include reconfigurable optical networks and advanced optical modulation formats.

Daniel C. Kilper (M'07–SM'07) was born in Chicago, IL, in 1968. He received the B.S. degree in electrical engineering and the B.S. degree in physics from Virginia Polytechnic Institute and State University, Blacksburg, in 1990, and the M.S. and Ph.D. degrees in physics from The University of Michigan, Ann Arbor, in 1992 and 1996, respectively.

Following his Ph.D. degree work, he was a Postdoctoral Research Scientist with the Optical Technology Center, Department of Physics, Montana State University. He became an Assistant Professor of physics with the University of North Carolina, Charlotte, in 1997. In 2000, he joined the Advanced Photonics Research Department, Bell Laboratories, Lucent Technologies, Holmdel, NJ, as a Member of Technical Staff. In 2006, he became a member of the Optical Networks Research Department, Bell Laboratories, Alcatel-Lucent. While at Bell Laboratories, he has conducted research on optical performance monitoring and transmission, architectures, and control systems for transparent and reconfigurable optical networks. He is an Associate Editor for the *Journal of Optical Networking*.

Dr. Kilper served on technical program committees for IQEC, Optical Technology in the Carolinas Conference, and was General Chair of the OPTO-Southeast Conference. He is currently serving on the Optical Communications Program Committees for CLEO/Europe and COIN/ACOFT. During 2003–2006, he was a member of the Bell Labs Advisory Council on Research. Since 2005, he has been the Bell Labs Ireland Photonics Deputy Strand Leader in the Center for Telecommunications Value Chain Research (CTVR).

Sethumadhavan Chandrasekhar (M'90–SM'00–F'01) received the B.Sc., M.Sc., and Ph.D. degrees in physics from the University of Bombay, Mumbai, India, in 1973, 1975, and 1985, respectively.

He is currently a Distinguished Member of Technical Staff in the Transmission Systems and Networking Department, Bell Labs, Holmdel, NJ. He was at the Tata Institute of Fundamental Research, Bombay, from 1975 to 1985 and at AT&T Bell Laboratories (later called Lucent Technologies, Bell Laboratories, and currently called Bell Labs, Alcatel-Lucent), Crawford Hill Laboratory, Holmdel, from 1986 to the present. He initially worked on compound semiconductor devices and high-speed optoelectronic integrated circuits (OEICs). Since January 1999, he has been responsible for forward-looking research in DWDM optical networking. His current interests include 40-Gb/s and 100-Gb/s transport and networking, modulation formats, and electronic signal processing at the receiver. He holds 18 U.S. patents.

Dr. Chandrasekhar is a member of the IEEE Lasers and Electro-Optics Society and has served as an Associate Editor of the IEEE PHOTONICS TECHNOLOGY LETTERS for more than ten years. He has been a member of the technical program committees of the IEDM, DRC, and OFC conferences. He was awarded the IEEE LEOS Engineering Achievement for 2000 and the OSA Engineering Excellence Award for 2004 for his contributions to OEICs and WDM systems research.

Liam P. Barry (M'98–SM'09) received the B.E. degree in electronic engineering and the M.Eng.Sc. degree in optical communications from University College Dublin, Dublin, Ireland, in 1991 and 1993, respectively. During the period 1993–1996, his research involved the use of ultrashort optical pulses in high-capacity optical networks, and as a result of this work he received the Ph.D. degree from the University of Rennes, Rennes, France.

From February 1993 to January 1996 he was a Research Engineer in the Optical Systems Department, France Telecom's Research Laboratories (CNET), Lannion, France. In February 1996 he joined the Applied Optics Centre, Auckland University, New Zealand, as a Research Fellow, and in March 1998, he took up a lecturing position in the School of Electronic Engineering, Dublin City University, where he established the Radio and Optical Communications Laboratory. His main research interests are high-speed optoelectronics devices, photonic systems, hybrid radio/fiber networks, and all-optical signal processing.